Recent results from ^{58}Ni+^{58}Ni @ 32, 52 and 74 MeV/nucleon analysis

Lucia Baldesi

FAZIA Days
4-5 February 2026

INDRA FAZIA

UNIVERSITÀ DEGLI STUDI FIRENZE

INFN
Istituto Nazionale di Fisica Nucleare

NUCLEX

Physics case

Heavy-Ion collision in the Fermi energy domain

Semiperipheral collisions at **intermediate energies** ($20 < E_{beam} < 100$ AMeV):

- **The dominant channel is the binary one:** formation of two excited fragments, which preserve memory of the entrance channel.

  In the ejectiles show a superposition of two effects:
  - **Statistical**: decay from a thermodynamically equilibrated source
  - **Dynamical**:
    - emission towards midvelocity → neck
    - neutron enrichment at midvelocity

- Another possible exit channel is the **dynamical breakup** of the QP and/or QT.

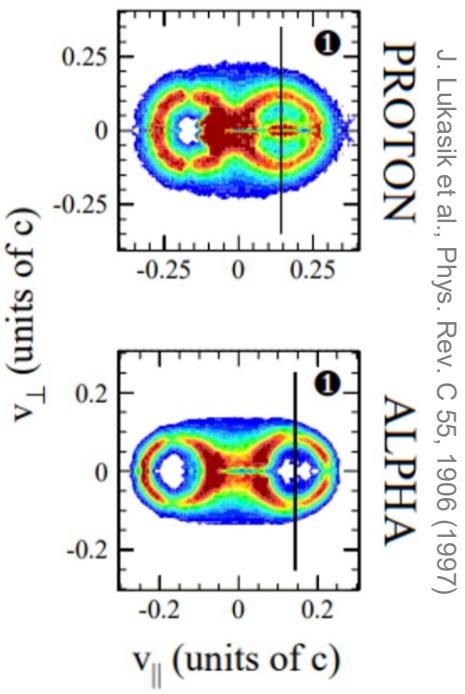

J. Lukasik et al., Phys. Rev. C 55, 1906 (1997)

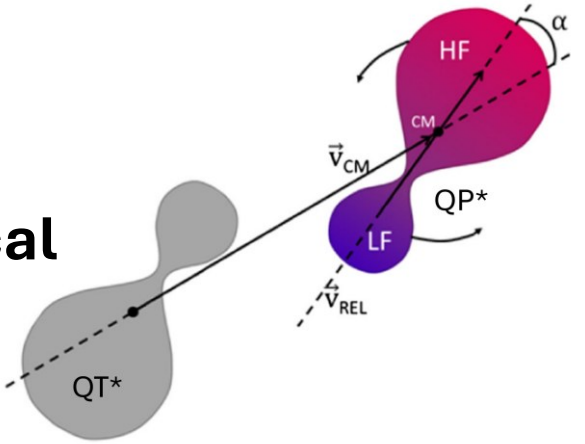

A. Jedele et al., Phys. Rev. Lett. 118, 062501 (2017)

BNV calculation of density contour plots

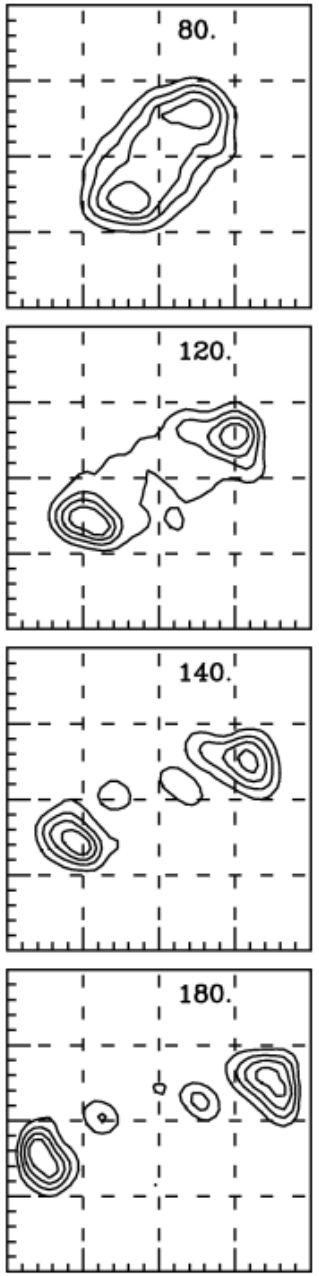

V. Baran et al., Nucl. Phys. A 703, 603 (2002).

Physics case

Heavy-Ion collision and the isospin drift

An experimental observation is the **neutron enrichment of the neck**, which can be interpreted in the framework of the **nuclear Equation of State**

V. Baran et al., Physics Reports 410 (2005) 335 – 466

$$\frac{E}{A}(\rho, I) = \frac{E}{A}(\rho) + \frac{E_{sym}}{A}(\rho) I^2$$

$$I = \frac{N - Z}{A}$$

$$\rho = \rho_n + \rho_z$$

Symmetric matter

Asymmetric matter

$$\frac{E}{A}(\rho) = E_{sat} + \frac{1}{2} K_{sat} x^2 + \ldots \qquad x = \frac{\rho - \rho_0}{\rho_0}$$

$$\frac{E_{sym}}{A}(\rho) = E_{sym} + L_{sym} x + \frac{1}{2} K_{sym} x^2 + \ldots$$

The symmetry energy produces a difference of the proton and neutron currents:

$$j_n - j_p \propto \frac{E_{sym}}{A}(\rho) \nabla I + \frac{\partial E_{sym}/A}{\partial \rho} \nabla \rho$$

Isospin Diffusion:

- driven by the isospin gradient
- tends to equilibrate neutron–proton imbalance.

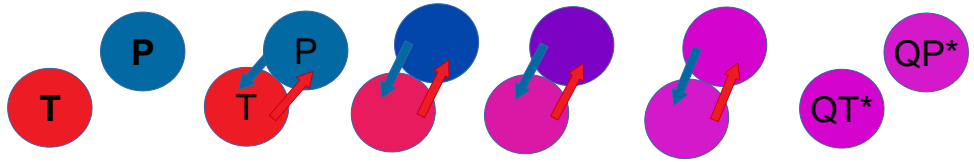

Isospin Drift:

- driven by the density gradient.
- induces a net neutron flux towards low density regions

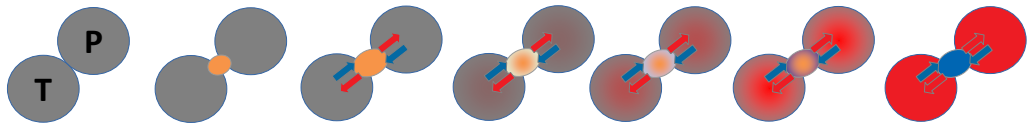

Physics case

^{58}Ni+^{58}Ni @ 32, 52 and 74 AMeV

^{58}Ni+ ^{58}Ni at 32, 52 and 74 AMeV :
(E789 and E818 experiments with INDRA-FAZIA apparatus)

evolution of the dynamics with incident energy and centrality in semipheripheral collisions

From the cold detected fragments, we aim to infer information on the dynamical phase:

- selection of the QP evaporative (**QPr**) and the QP breakup (**QPb**) channels
- **Primary source reconstruction**: size and excitation energy of the primary QP* and the neck source
- **Isospin drift:** isospin investigation of the evaporative and midvelocity emissions

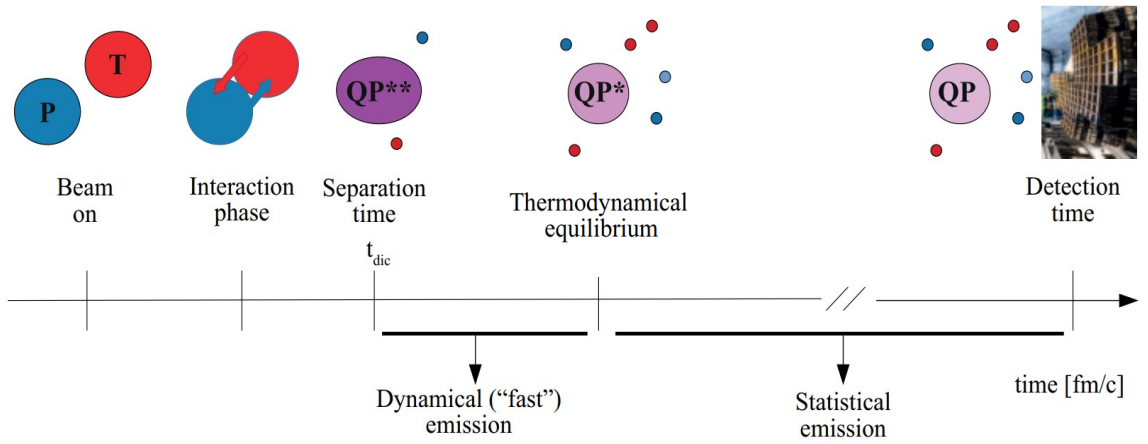

Data selection

NOTE:
- Light fragments: Z≤4
- Big fragments: Z>4
- QP fragments: Z>14

- events with M≥2 in FAZIA
- channels of interest
  - QPr channel
    - $M_{BF}=1$
    - $Z_{BF}>14$
    - v_z^{cm} (BF)>0

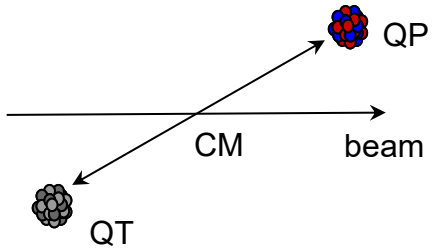

  - QPb channel
    - $M_{BF}=2$
    - $Z_{rec}= Z_{HF}+Z_{LF} >14$
    - v_z^{cm} (rec)>0
    - $\theta_{rel} < \theta_{max}$
    - 12 mm/ns < v_{rel} < v_{max}

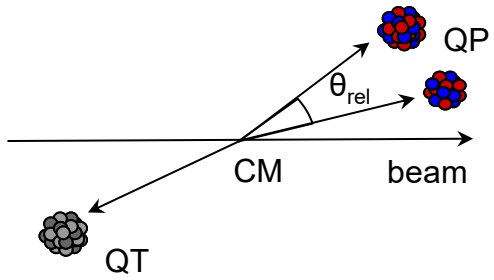

- Centrality estimator:
  reduced momentum $p_{red}= \left(\frac{p_z^{QP}}{p_{beam}}\right)$

QP (detected or reconstructed) fragments

QPr channel

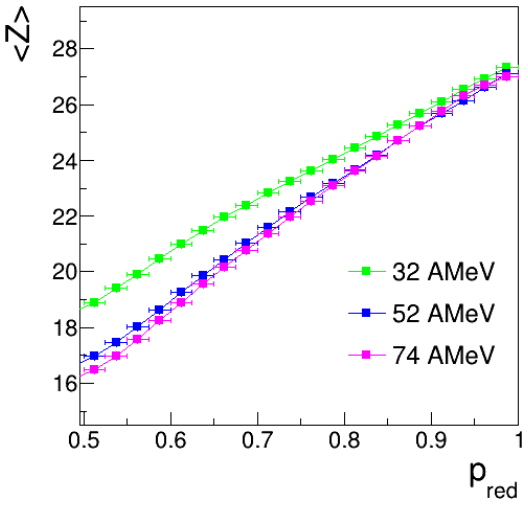

QPb channel

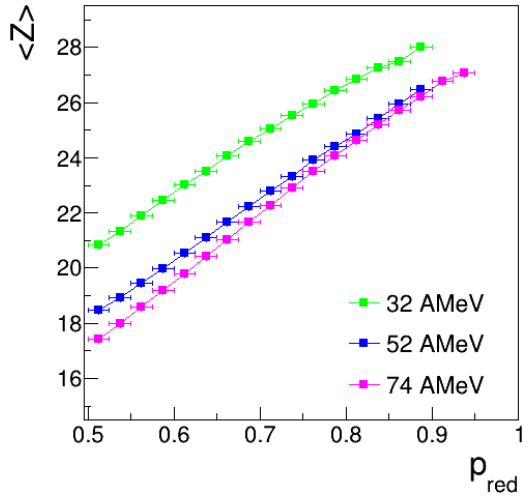

- <Z> of QP fragments :
  - depends on centrality and beam energy
  - the reconstructed QP in the breakup channel is on average larger than the remnant QP in the evaporation channel

32 AMeV

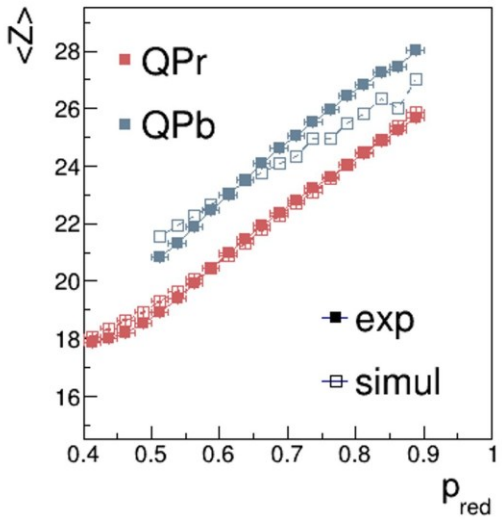

52 AMeV

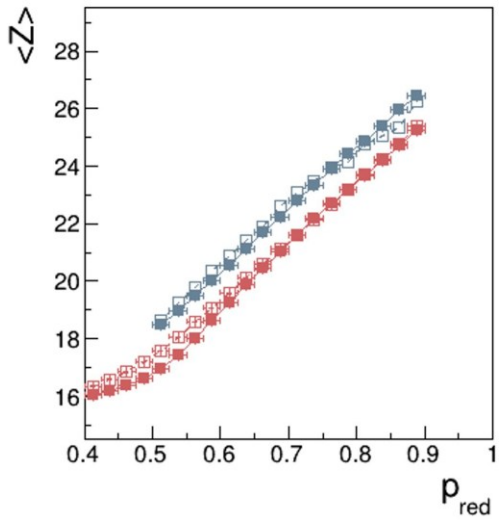

74 AMeV

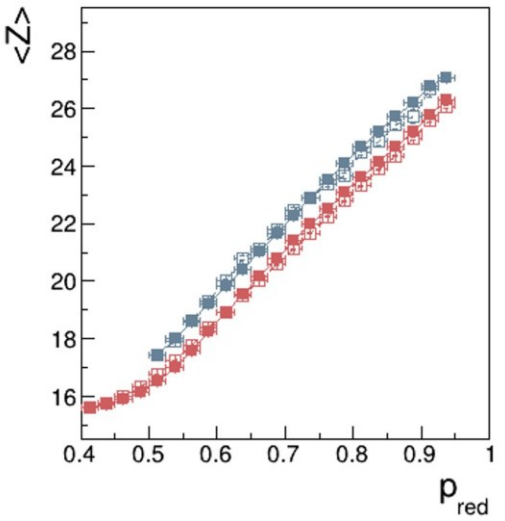

Light fragments (Z<5)

- selection of fragments (**identified in mass**) emitted in the **forward hemisphere of the center of mass reference frame**
  - $v_{\parallel}^{cm} > 0$, where $v_{\parallel}^{cm}$ is the velocity component along the asymptotic QP-QT axis in the center of mass reference frame

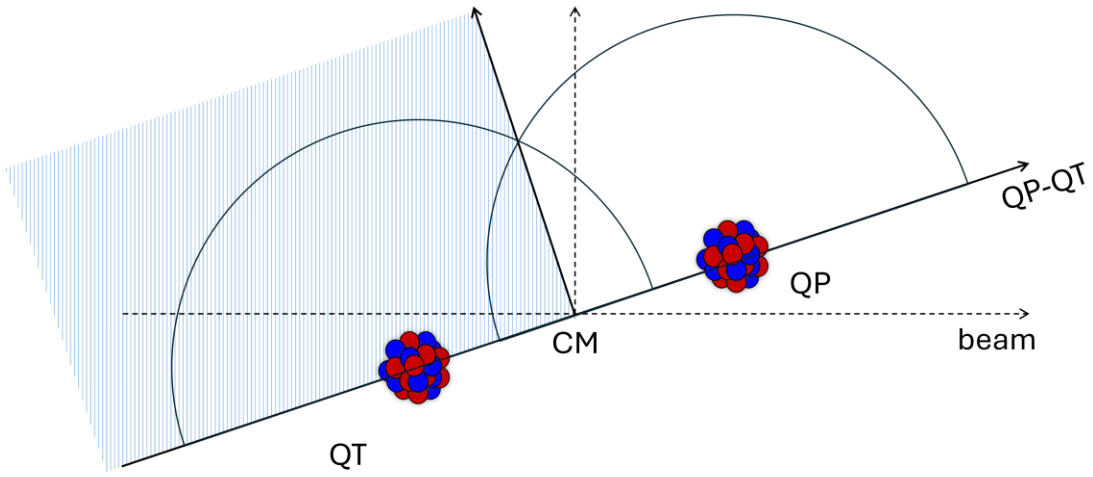

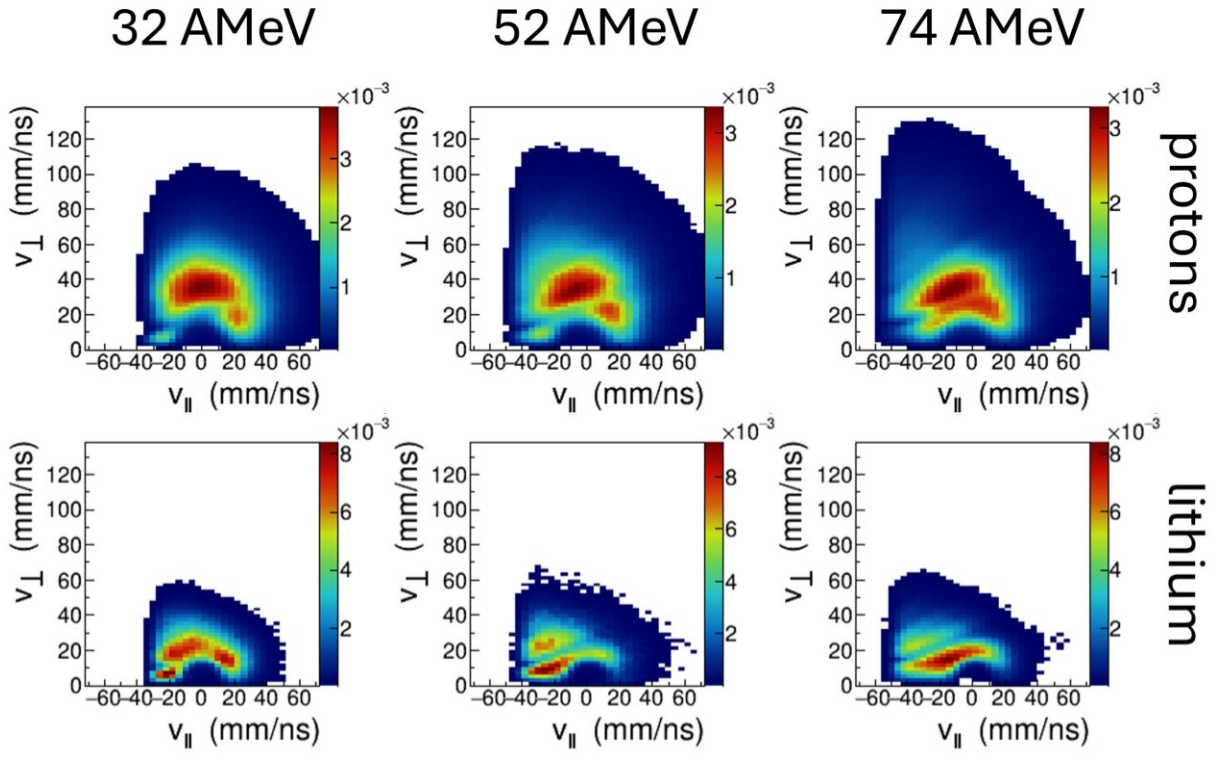

Experimental yields in the $(v_{\parallel}, v_{\perp})$ plane

- parallel and perpendicular components, with respect to the asymptotic QP-QT axis, of velocity in the QP reference frame
- to properly account for relativistic kinematics, $v_{\parallel}$ and $v_{\perp}$ are actually the rapidity y and the transverse velocity $\beta_{\perp}$ multiplied by c.

Efficiency correction

Efficiency correction for light fragment multiplicities:

- obtained using AMD+GEMINI++ simulations for all incident energies
  - average correction factors for each bin of p_{red} and for each cell in the $(v_{\parallel}, v_{\perp})$ velocity space
  - Z = 1 particles: separate correction factors for each isotope
  - Z > 1 particles: a correction factor for each element.
- proton multiplicities further corrected to account for IED events in the FAZIA CsI detectors
- comparison between experimental multiplicities corrected with AMD+GEMINI++ and HIPSE for the reaction at 74 AMeV
  - the differences depend on both the particle species and the centrality, and they can reach up to 10%

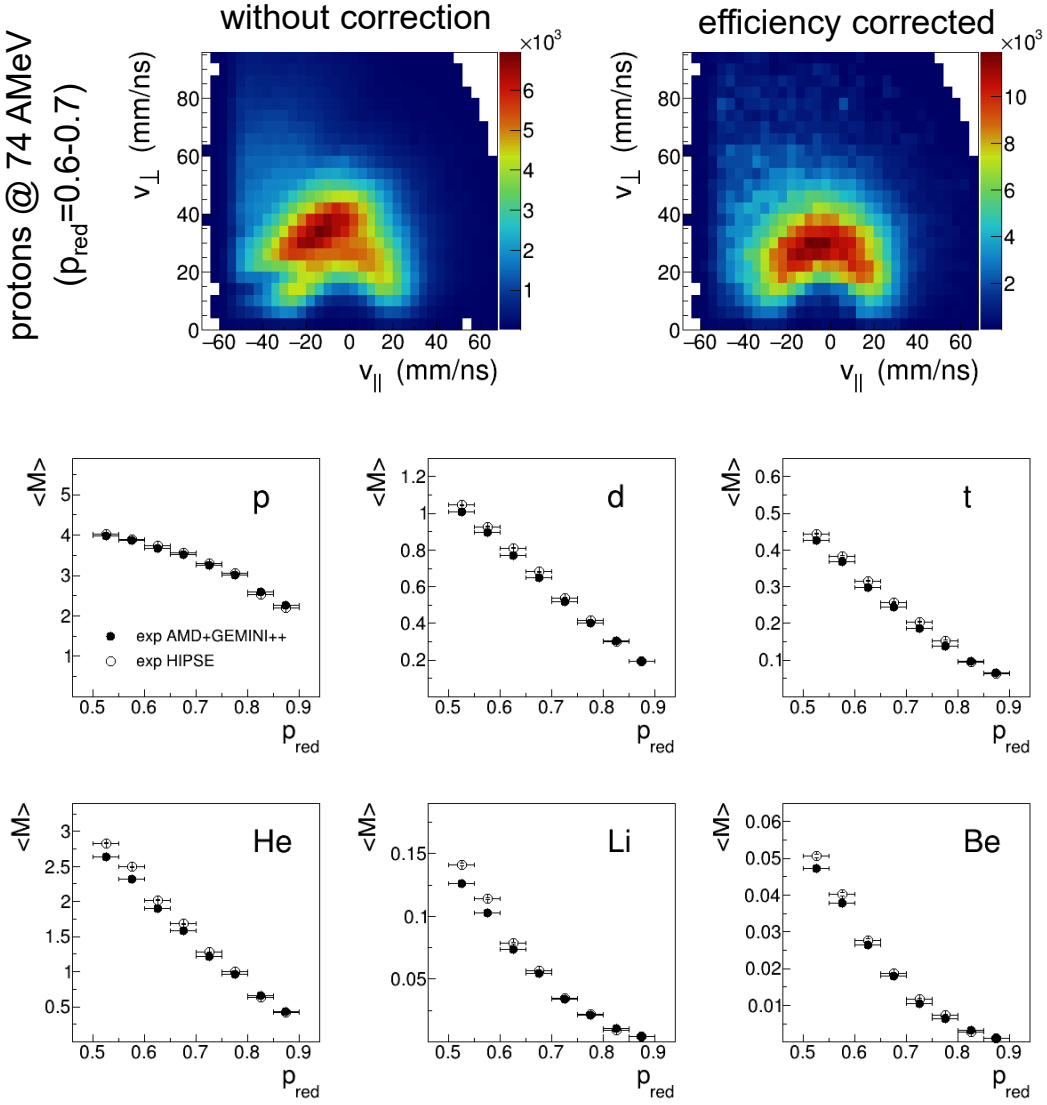

Efficiency check and free neutron estimation

- the quality of the efficiency correction was validated by comparing the average total forward-emitted charge and the projectile charge.
- the projectile charge is well reproduced, within about one charge unit.

QPr channel ^{58}Ni+^{58}Ni @ 74 AMeV

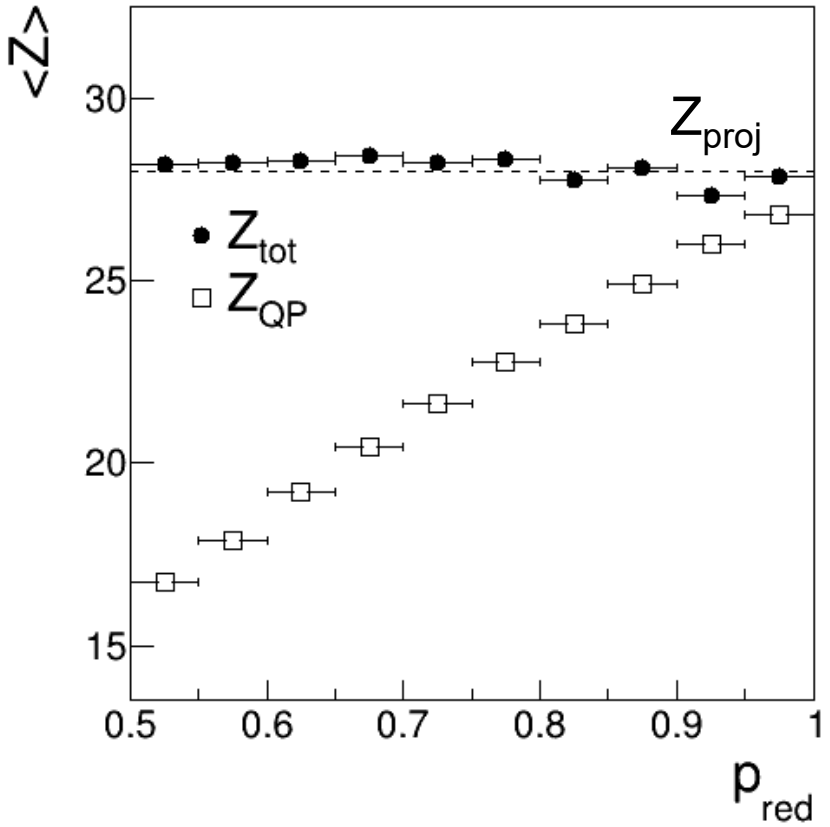

- free neutrons are not detected, preventing the recovery of the initial projectile neutron number
- free neutron multiplicity was estimated from conservation law, as the difference between the Nprojectile and the total number of bounded neutrons.

QPr channel ^{58}Ni+^{58}Ni @ 74 AMeV

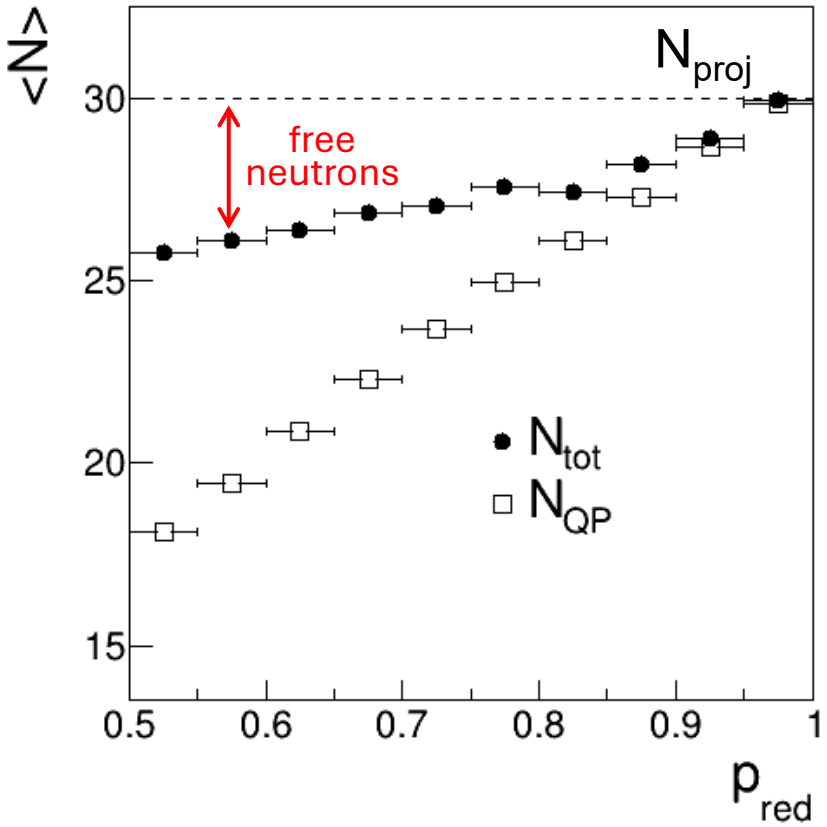

Disentanglement of evaporative and midvelocity emissions

S. Piantelli, PRC 74, 034609 (2006)
A. Mangiarotti, PRL 93, 232701 (2004)

- **Light charged fragments:**
  - angular distributions of θ, i.e. the polar angle between the charged particle in the QP frame and the QP-QT separation axis
    - → superposition of two emission components
      - **statistical evaporation**: approximately a sin(θ) distribution → sin(θ) fit in the angular range 0°<θ<45°.
      - large excess at backward angles which is ascribed to **midvelocity emission**.

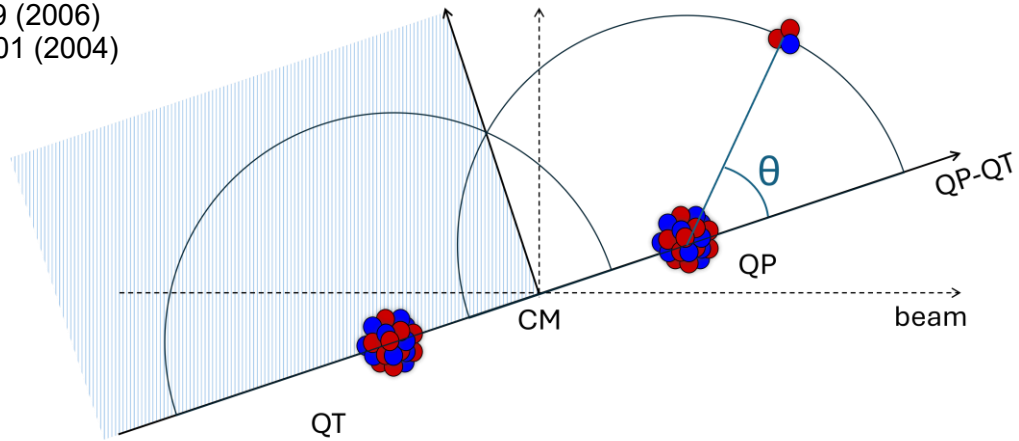

- **Free neutrons**
  - an assumption must be made:
    - the neck region has the same N/Z ratio as the overall system (i.e. 1.07).
    - uncertainty estimated by varying the assumed N/Z value of the neck within a reasonable range, from 0.97 to 1.17

^{58}Ni+^{58}Ni @ 74 AMeV

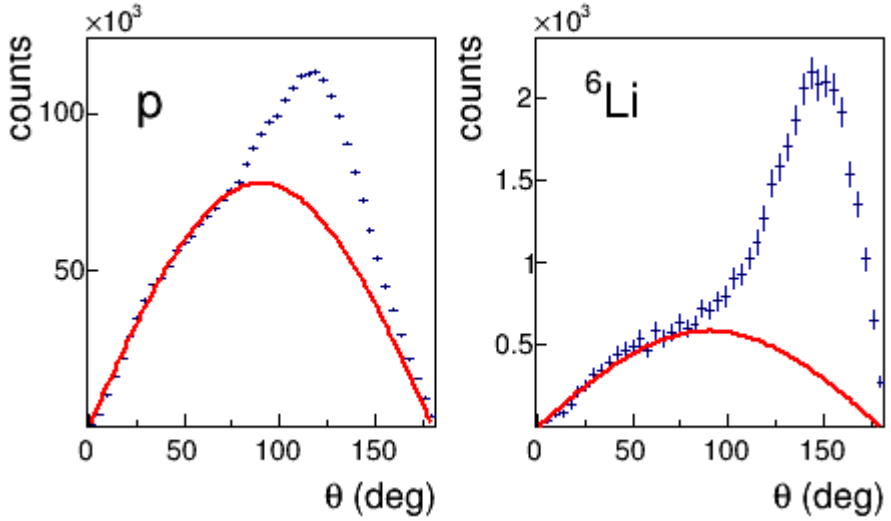

Primary sources: charge/mass

primary QP*

QPr channel

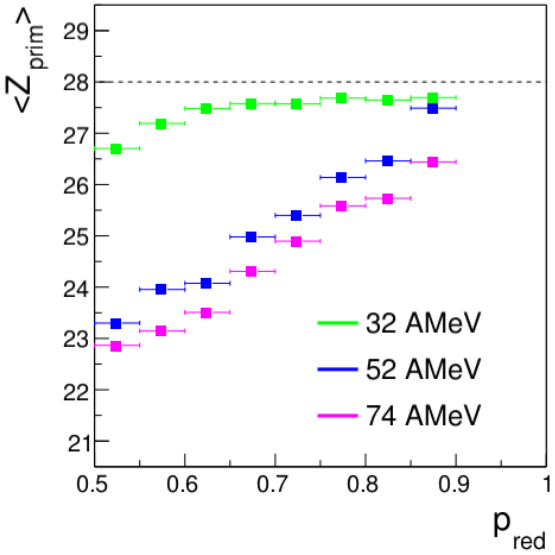

QPb channel

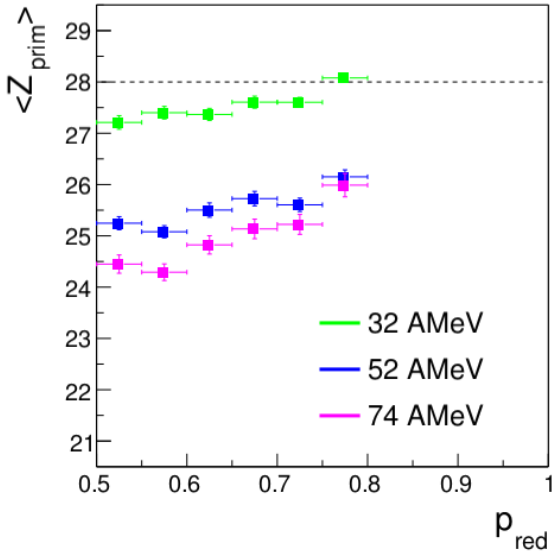

- the size of the QP* depends on both centrality and incident energy

forward-emitted midvelocity (half neck*)

QPr channel

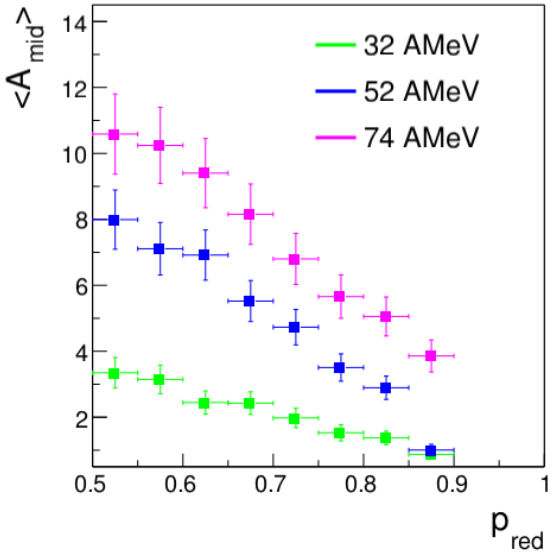

QPb channel

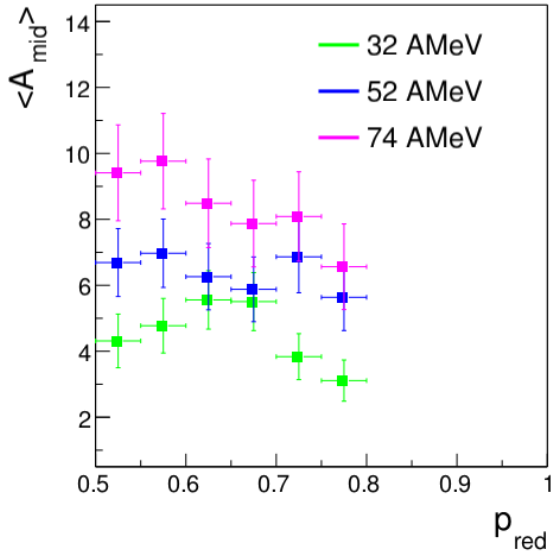

- the midvelocity contribution grows with centrality and beam energy

* quantities refer to forward-emitted particles; owing to the symmetry of the system, the total neck mass is twice the reported values, while its energy density can be considered representative of the entire neck emission.

Primary sources: excitation energy

primary QP*

QPr channel

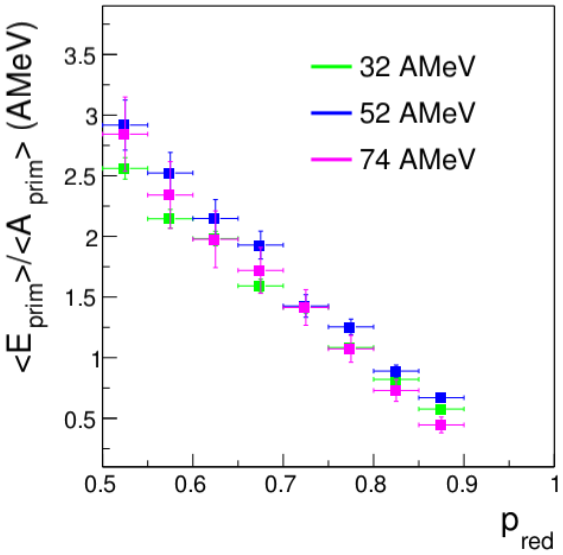

QPb channel

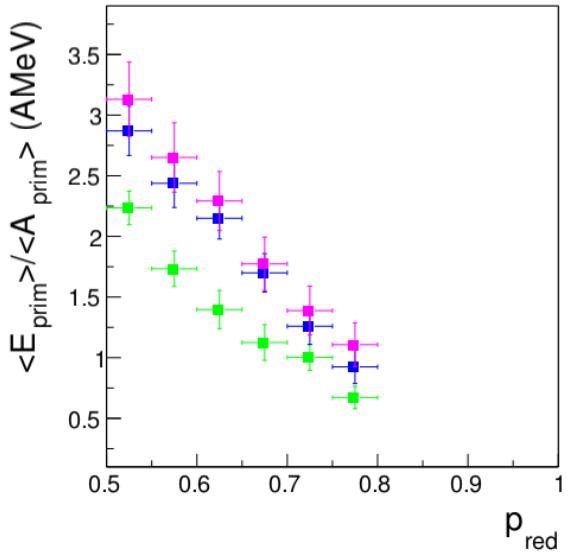

- increases with centrality
- below 3 MeV/nucleon

forward-emitted midvelocity (half neck*)

QPr channel

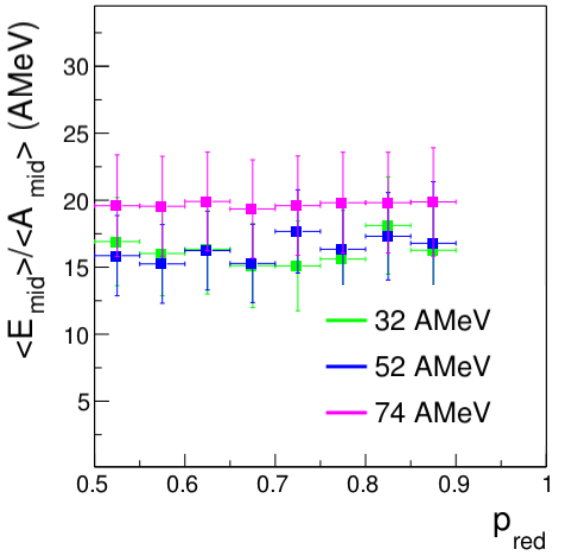

QPb channel

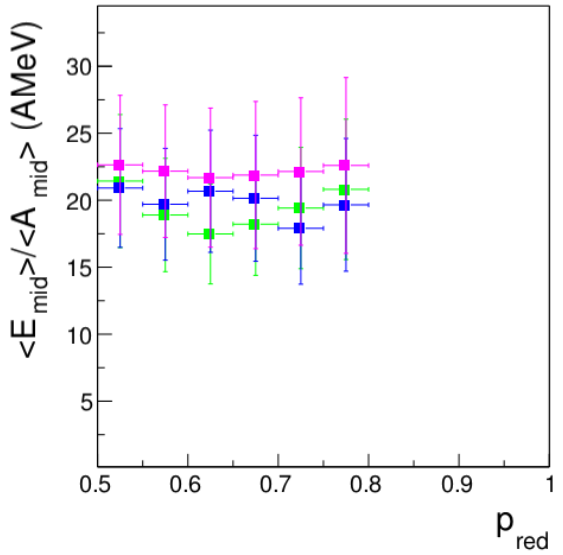

- not straightforward to associate this energy density with the thermal excitation energy of a defined nuclear source
- ~ 15-20 MeV/nucleon
- no dependence on either centrality or beam energy.

* quantities refer to forward-emitted particles; owing to the symmetry of the system, the total neck mass is twice the reported values, while its energy density can be considered representative of the entire neck emission.

Primary sources: comparison with AMD+GEMINI++

primary QP*

forward-emitted midvelocity (half neck*)

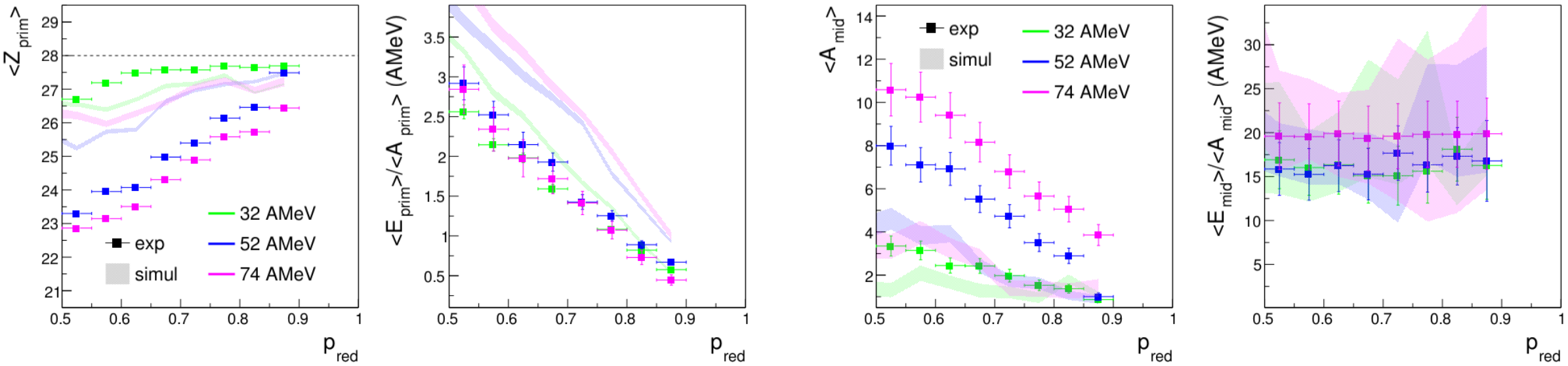

- overall satisfactory reproduction of the secondary fragment characteristics
- underestimation of the midvelocity contribution at higher beam energies
- the reconstructed QP* sources appear hotter and heavier than experimental ones

* quantities refer to forward-emitted particles; owing to the symmetry of the system, the total neck mass is twice the reported values, while its energy density can be considered representative of the entire neck emission.

Primary sources: systematic uncertainties

- efficiency correction
  - comparison between experimental data corrected using AMD+GEMINI++ and HIPSE
  - good agreement with only minor deviations (< 1 charge unit) for $\langle Z_{prim} \rangle$
  - this confirms the robustness of the efficiency correction procedure, with an associated systematic uncertainty of ~5%

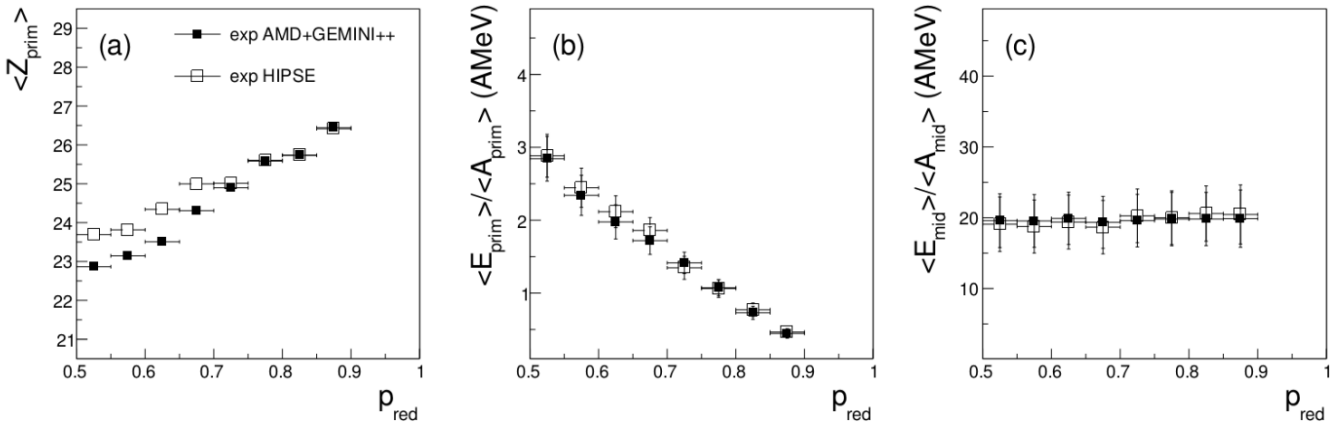

- Pre-equilibrium
  - the pre-equilibrium emission was not explicitly considered
  - one may wonder to what extent this component could affect the results
    - ■ it predominantly affects protons (and neutrons)
    - ■ even in the worst case, its contribution does not exceed ~15%,
    - → a systematic uncertainty can be roughly estimated to be below 2-3%.

Experimental proton kinetic energy spectra in the QP reference frame for $10°<\theta<20°$ for p_{red}=0.65-0.70

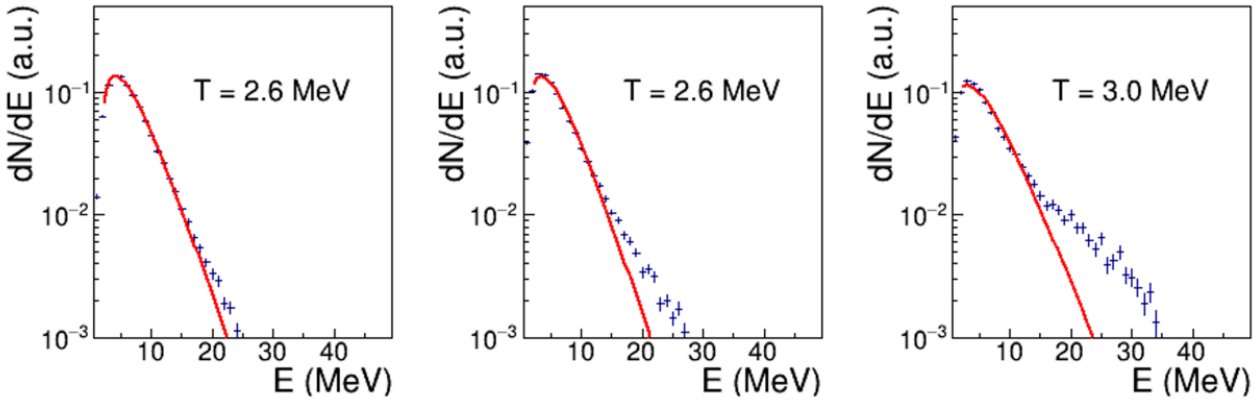

Isospin analysis

isospin ratio for complex particles:

$$\langle N\rangle/\langle Z\rangle_{CP} = \frac{\sum_i \sum_\nu N_\nu^i}{\sum_i \sum_\nu Z_\nu^i}$$

E. Galichet, PRC 79, 064614 (2009)

- outer sum over all events belonging to a given p_{red} bin
- inner sum over all complex particles ν (Z<5 and A>1) detected in the i-th event
- free protons and neutrons are excluded

QPr channel

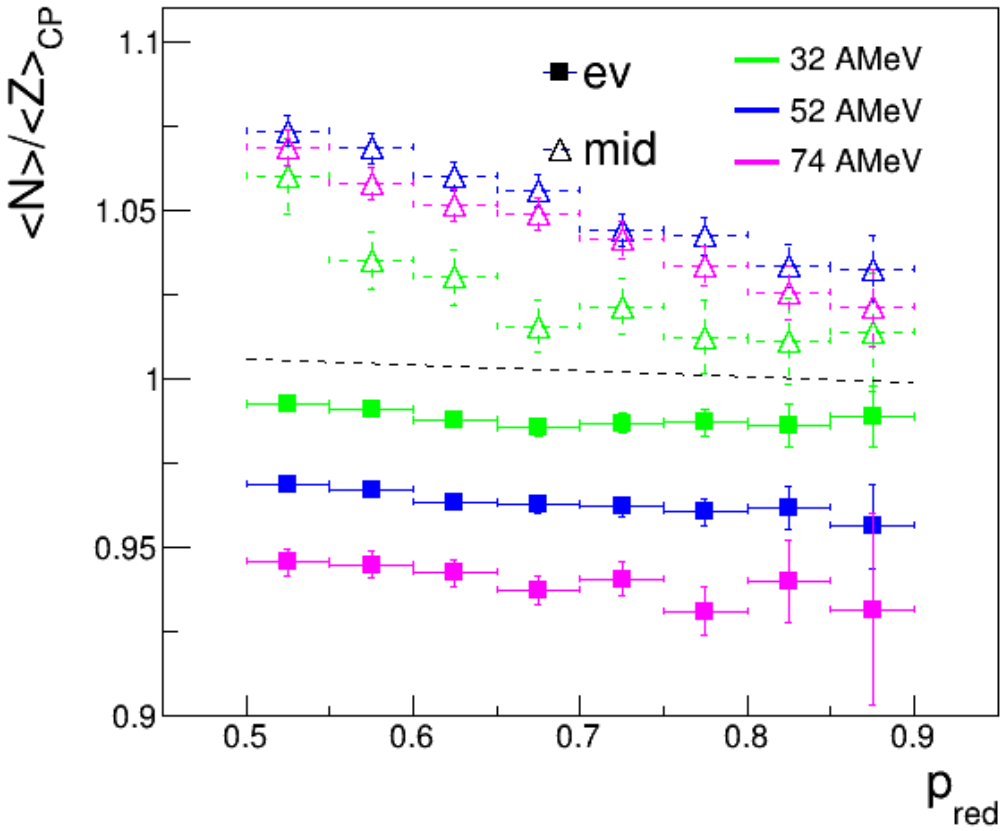

- midvelocity component exhibits a systematically larger $\langle N\rangle/\langle Z\rangle_{CP}$ than the evaporative component: the **neutron enrichment of the neck** is clearly observed
- N/Z of the midvelocity emission is almost independent of the beam energy.
- N/Z of evaporative component displays an ordering as a function of incident energy
  - reflects a different isospin content of the QP* source
  - effect related to an increasing contribution of midvelocity emission at higher energies

Isospin analysis

QPr channel

isospin ratio for complex particles
(free protons and neutrons excluded)

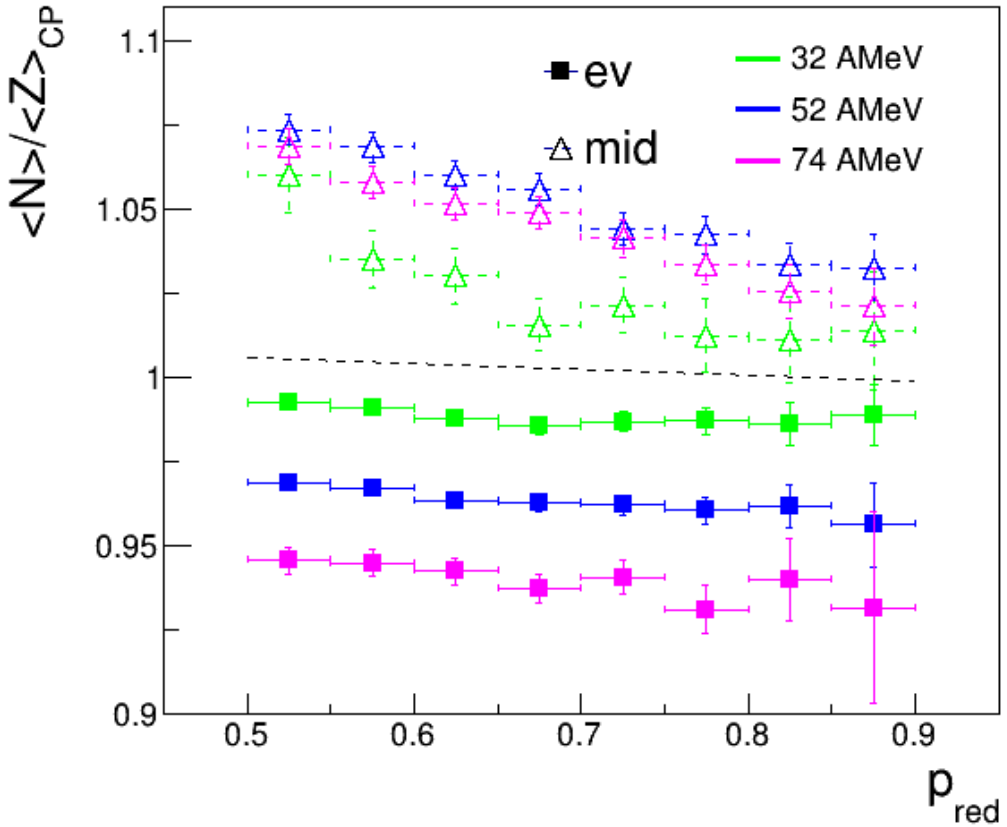

average mass of Z=1 isotopes

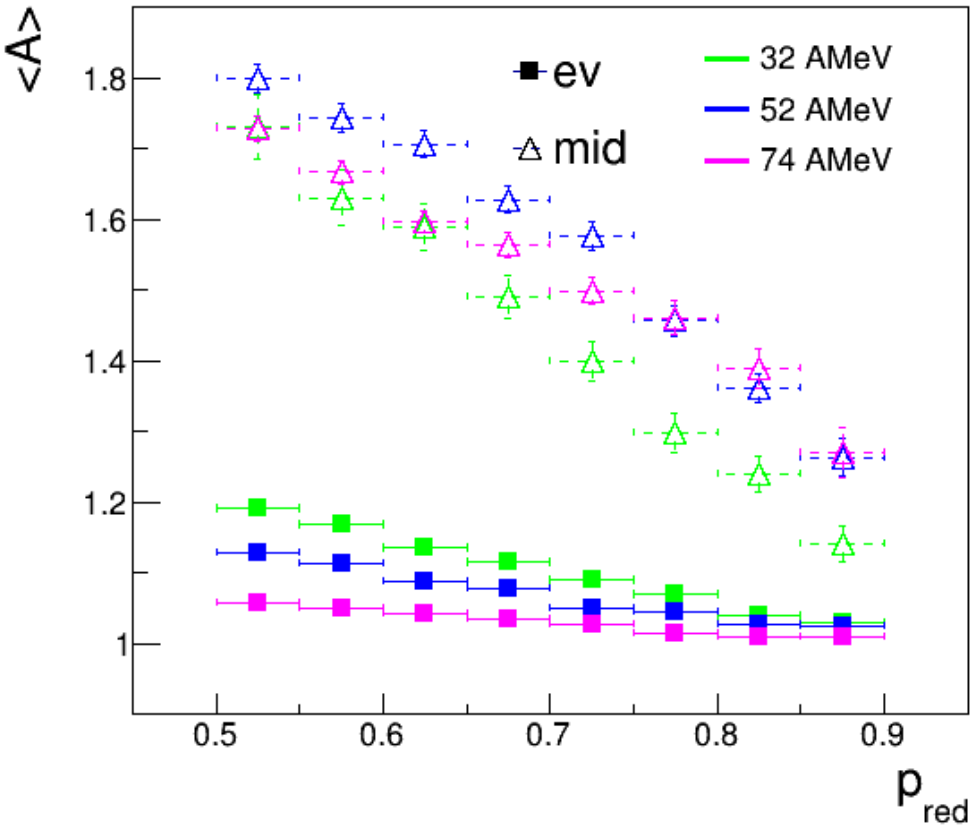

- inclusion of previously excluded protons
- similar observation reinforcing the previous finding

Isospin analysis: QPr vs QPb channels

isospin ratio for complex particles

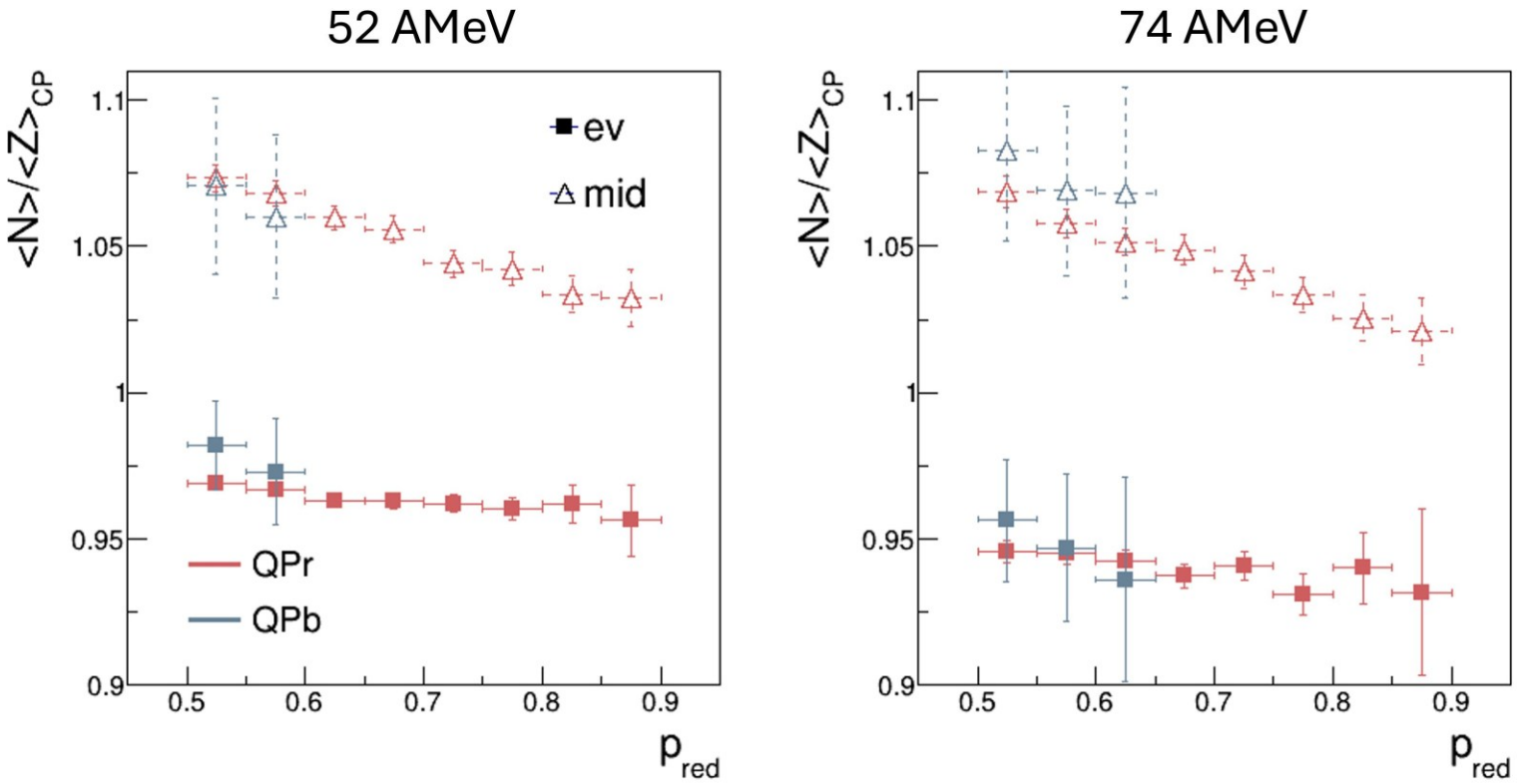

- limited due to the lower statistics
- similar results as the QPr channel

Summary and conclusions

Experimental investigation of the **reaction dynamics** of semiperipheral **^{58}Ni+^{58}Ni** collisions at **32,52 and 74 AMeV** in the QPr and QPb channels

- **Primary source reconstruction**
  - Similar results in the QPr and QPb channels
  - the excitation energy of the primary QP* remains below 3 AMeV
  - the midvelocity contribution increases with increasing incident energy
  - the energy density of the neck source is 15-20 AMeV → dynamical origin from a hot overlapping region
  - the systematic uncertainty related to the efficiency correction is estimated to be below ~5%.
  - a rough estimation of the pre-equilibrium emission suggests a systematic error below 2–3%.
  - AMD+GEMINI++ simulations, while reproducing well the characteristics of the secondary QP, fail to reproduce those of the primary QP*, as they underestimate the midvelocity contribution.
  - simulation results indicate that the sources reconstructed through the proposed procedure correspond to reaction times of approximately 150-300 fm/c from the onset of the collision

- **Isospin Drift**
  - a clear neutron enrichment of the neck region is observed at all incident energies
  - the midvelocity contribution plays a role in determining the isospin content of the primary QP* and consequently influences that of the evaporated particles